Learning to Predict Video Saliency using Temporal Superpixels

Anurag Singh[1], Chee-Hung Henry Chu[1,2] and Michael A. Pratt[3]
[1]*Center for Advanced Computer Studies, University of Louisiana at Lafayette, Lafayette, LA, U.S.A.*
[2]*Informatics Research Institute, University of Louisiana at Lafayette, Lafayette, LA, U.S.A.*
[3]*W.H. Hall Department of Electrical and Computer Engineering,University of Louisiana at Lafayette, Lafayette, LA, U.S.A.*

Keywords: Video Saliency, Temporal Superpixels, Support Vector Machines, Saliency Flow.

Abstract: Visual Saliency of a video sequence can be computed by combining spatial and temporal features that attract a user's attention to a group of pixels. We present a method that computes video saliency by integrating these features: color dissimilarity, objectness measure, motion difference, and boundary score. We use temporal clusters of pixels, or temporal superpixels, to simulate attention associated with a group of moving pixels in a video sequence. The features are combined using weights learned by a linear support vector machine in an online fashion. The temporal linkage for superpixels is then used to find the saliency flow across the image frames. We experimentally demonstrate the efficacy of the proposed method and that the method has better performance when compared to state-of-the-art methods.

1 INTRODUCTION

Finding what attracts a viewer's attention in video data has many applications in video analysis and pattern recognition, such as video summarization, video object recognition, surveillance, and compression. In these applications, it is paramount to find the salient object in the video. A majority of work in predicting video saliency focuses on eye tracking where the aim is to mimic human vision. The major problem associated with eye-tracking saliency maps is that they do not scale well with higher level applications (Cheng *et al*., 2011), such as object detection. In this paper we propose a new method to detect salient objects in a video sequence using feature integration theory.

Treisman and Gelade (1980) in their seminal work described feature integration theory in which visual attention is derived from many features in parallel. These features are combined together linearly to focus where the attention is at a salient location. The weights in the combination step rank the features according to their relative importance.

Building on this biological principle we propose to use four features which attract attention in parallel. These features are: (i) color contrast, which is the most discriminant feature to differentiate a salient vs non-salient region; (ii) motion difference, which captures the change in the location of a salient object; (iii) notion of objectness*,* which gives the probability of occurrence of a generic object; and (iv) boundary score, which is a measure of the existence of boundary. In our method, the feature combination step is achieved by learning the weights using a linear support vector machine.

In a dynamic scene depicted in a video sequence, the focus of attention tends to occur in clusters (Mital *et al*., 2011) rather than at the pixel level. Clustering of pixels into meaningful homogeneous regions forms what are referred to as superpixels. Temporal coherence between superpixels so that the same superpixel belongs to same object across the frames is accomplished by using temporal superpixels (Chang *et al*., 2013).

The feature integration technique described above finds the fixation in a single frame and in principle we could just find attention separately for every frame. Saliency detection for a single image (frame) differs from that for video in that the viewer has no continuous or prior information when viewing a single image, so that there is no gaze transition. In video saliency detection prior information is essential to facilitate the gradual transition of attention from one region of importance to another over several frames. Transition from a single frame to video is modeled by online learning of weights and by using prior saliency information from the previous frames to update the current frame via a saliency flow framework.

Singh A., Henry Chu C. and A. Pratt M..
Learning to Predict Video Saliency using Temporal Superpixels.
DOI: 10.5220/0005206402010209
In *Proceedings of the International Conference on Pattern Recognition Applications and Methods* (ICPRAM-2015), pages 201-209
ISBN: 978-989-758-077-2

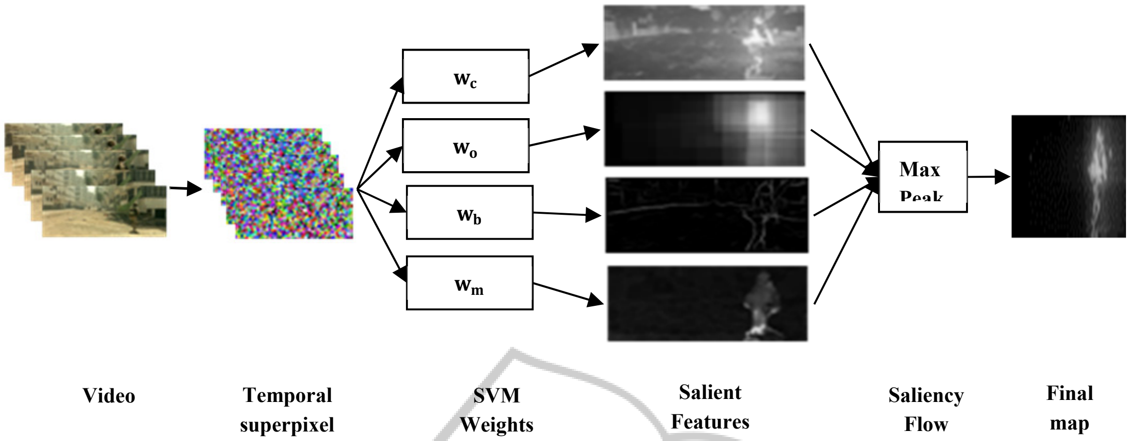

Figure 1: Flow diagram for detecting video saliency.

2 RELATED WORK

Itti and Baldi (2005) use the feature integration theory to combine local cues of intensity, color, orientation, motion in parallel using a center surround map. A surprising change to a distribution is captured by maximizing the posterior probability of the combination map. Mahadevan and Vasconcelos (2010) use a biologically inspired discriminant center surround saliency hypothesis for video where each pixel is represented by a spatio-temporal patches which is contrasted with the center to find saliency. Using rare or abnormal motion to detect saliency in a video is proposed by Mancas *et al.* (2011) where only dynamic features are used and no static features such as color or contrast are incorporated. Fukuchi *et al.* (2009) use a stochastic representation of saliency map using Kalman filters.

Rudoy *et al.* (2013) present a method to predict the gaze location given the previous frame fixation map. They generate three sets of candidate maps as static, semantic and motion maps. A random forest classifier is trained to predict the location of the gaze in the next frame. Our method extends their work in that we use a learning-based feature integration along with a Gaussian process-based superpixel linkage (Chang *et al.,* 2013) to generate video saliency.

3 VIDEO SALIENCY

3.1 Temporal Superpixels

As fixation occurs in clusters it is useful to group pixels together into regions. The so-called superpixels are one way to do this grouping. Ren and Malik (2003) use Gestalt principles for grouping pixels into superpixels where a good grouping meant that each group confirms to proximity, similarity and homogeneity. Extension to video requires solving that superpixel correspondence (Figure 2) that entails ensuring a superpixel's boundary remains constant in subsequent frames under the constraints of change in intensity, occlusion, camera movement and deformation.

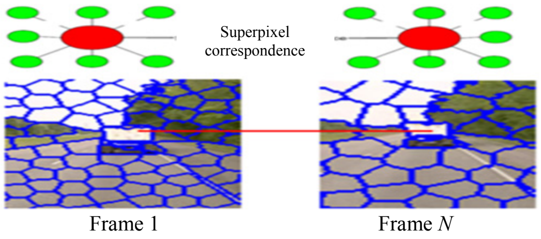

Figure 2: Temporal Superpixel Representation showing superpixel correspondence.

There are existing methods for solving the superpixel correspondence problem. Xu and Carso (2012) provide an excellent review for supervoxels based methods that extend superpixels to supervoxels in video frames. A supervoxel can be generated using the mean shift method (Paris and Durand 2007), a graph based method (Grundmann *et al.,* 2010), segmentation by weighted aggregation (Sharon *et al.,* 2006), an energy optimization framework (Veksler *et al.,* 2010), or superpixels rates for color histogram (Van den Bergh *et al.,* 2013). Supervoxels are over-segmented but not regular sized so that the boundaries do not remain the same.

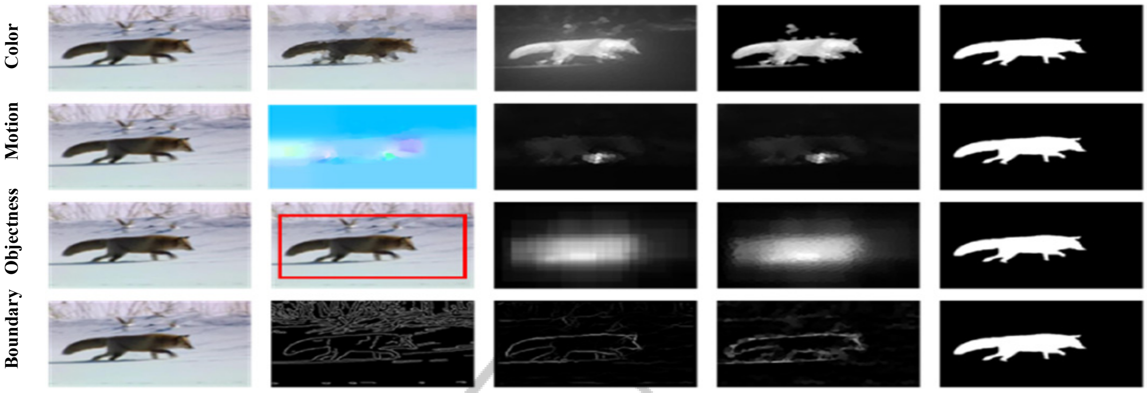

Figure 3: Feature Maps. Rows indicates features map associated with color, motion, objectness and boundary while column shows input; intermediate level details (for color it is average color, for motion it is optical flow, for objectness it is bounding box and for boundary it is edge map); pixel-level details; superpixel-level details; and ground truth.

To extend superpixels in its basic form for videos, temporally consistent superpixels create a global color space and superpixels are assigned to the color space depending on an energy function and the mutability of the sliding window frame (Reso *et al.*, 2013). In temporal superpixel, a temporally linked superpixel is created in each frame by building a generative graphical model using topological constraints (Chang *et al.*, 2013). We use temporal superpixels as it gives regular shaped compact superpixels with intact boundaries across frames.

3.2 Salient Features

Salient features are those which attract attention. In our work, they are color dissimilarity, motion difference, objectness, and boundary score. Figure 3 shows the feature maps computation at different stages.

3.2.1 Color Dissimilarity

Color dissimilarity is measured by comparing the color difference between superpixels. A group of pixels is dissimilar with respect to other pixel groups if it stands out (Goferman *et al.*, 2010). The dissimilarity for a pair of superpixels is given by Singh *et al.* (2014) as

$$d(sp_i, sp_j) = \frac{dcolor(sp_i, sp_j)}{1 + dposition(sp_i, sp_j)} \qquad (1)$$

where $dcolor(sp_i, sp_j)$ is the color difference between superpixels computed as the distance between two average colors in the CIE $L^*a^*b^*$ color space and $dposition(sp_i, sp_j)$ is the position difference between superpixel centers. The CIE $L^*a^*b^*$ color space is used because it supports chromatic double opponency. Further, we aggregate the individual dissimilarities as follows,

$$Gsp_i = \frac{1}{n}\sum_{j=1}^{n} d(sp_i, sp_j) \qquad (2)$$

where Gsp_i is the global dissimilarity measure for superpixel i, n is the number of superpixels and $d(sp_i, sp_j)$ is the local dissimilarity measure from Equation 1. The global dissimilarity measure is mapped to the saliency feature so that the higher the global dissimilarity measure, the closer the saliency is to 1. In our work, the color dissimilarity map is given by $color_i = 1 - \exp(-Gsp_i)$.

3.2.2 Motion Difference

A change in motion attracts attention; to capture this change we compute motion difference between frames. At frame *t*, we first compute the optical flow (Sun *et al.*, 2010) to obtain at each pixel location the horizontal and vertical velocity components denoted, respectively, $u_t(x,y)$ and $v_t(x,y)$. We compute the changes in velocity components as $\Delta u_t = u_{t-1} - u_{t-2}$ and $\Delta v_t = v_{t-1} - v_{t-2}$. The frame motion difference is determined in terms of these changes:

$$f_t(x,y) = \sqrt{(\Delta u_t(x,y))^2 + (\Delta v_t(x,y))^2} . \qquad (3)$$

The motion difference for superpixel *r* is given by

$$motion_r = \frac{1}{J}\sum_{j=1}^{J} f_{r,t}(x_j, y_j) \qquad (4)$$

where J is the total number of pixels in the

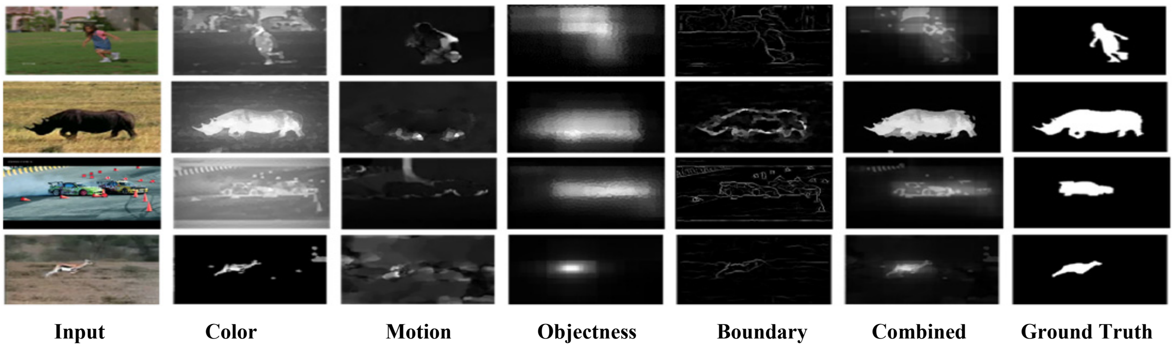

Figure 4: Individual features and integrated results (“Combined”) compared to Ground Truths.

superpixel and $f_{r,t}$ are pixels in superpixel r at frame t. The motion difference ensures only fast moving pixels which generate strong cues have a stronger contribution towards saliency detection.

3.2.3 Objectness Measure

Human eyes are most tuned to be fixated on an object in a scene. There can be one or many salient objects in an image that can be anywhere in the scene. The objectness map of an image is the probability of occurrence of an object in a window (Alexe *et al.*, 2012). Sampling for object windows gives the notion of objectness (Sun and Ling, 2013), which ensures a higher probability value for the occurrence of an object. Objectness for a superpixel is computed by finding the average objectness of underlying pixels in a superpixel as follows:

$$objectness_r = \frac{1}{J}\sum_{j=1}^{J} Pob_r(x_j, y_j) \tag{5}$$

where $objectness_r$ is the objectness for superpixel r, J is the total pixels in superpixel r, Pob_r is the probability of occurrence of an object in objectness map (Sun and Ling 2013), and x_j, y_j is the location of the *j*th pixel.

3.2.4 Boundary Score

Boundaries encompass both edges and corners in a way that is more natural to human perception. Not all edges attract attention but those pixels that do attract attention often lie on a boundary. We calculate a boundary score as a measure of how likely a pixel is a boundary pixel. For boundary detection we use the learned sparse code gradients (Ren and Bo 2012). The boundary score of superpixel r is given by

$$boundary_r = \frac{1}{J}\sum_{j=1}^{J} gPB_r(x_j, y_j) \tag{6}$$

where J is the total pixels in superpixel r, gPB_r is the boundary map of the image (Ren and Bo, 2012), and x_j, y_j is the location of the *j*th pixel.

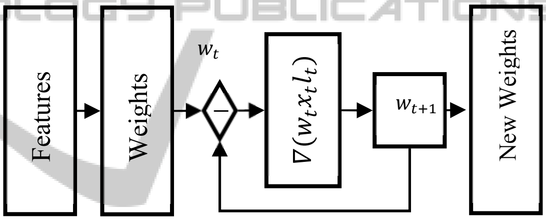

Figure 5: Online update of weights.

3.3 Feature Integration using SVM

The value of superpixel r in a saliency map, denoted S_r, is formed by a linear combination of the salient features:

$$\begin{aligned} S_r &= w_c color_r + w_o objectness_r \\ &\quad + w_m motion_r + w_b boundary_r \end{aligned} \tag{7}$$

where the weights w_c, w_o, w_m, w_b are found by the linear support vector machines (SVM) (Chang and Lin, 2008). In the following, when we compute the saliency value in a video sequence, we refer to the saliency value for the rth superpixel in the τth frame as $S_{r,\tau}$.

A linear SVM when given a training set (x_i, l_i), $x_i \in R^n, l_i \in \{1, -1\}, i = 1, \dots, N$, solves the following unconstrained problem:

$$\min_{w,b} \frac{1}{2} w^T w + C \sum_{i=1}^{N} \xi(w, b; x_i, l_i) \tag{8}$$

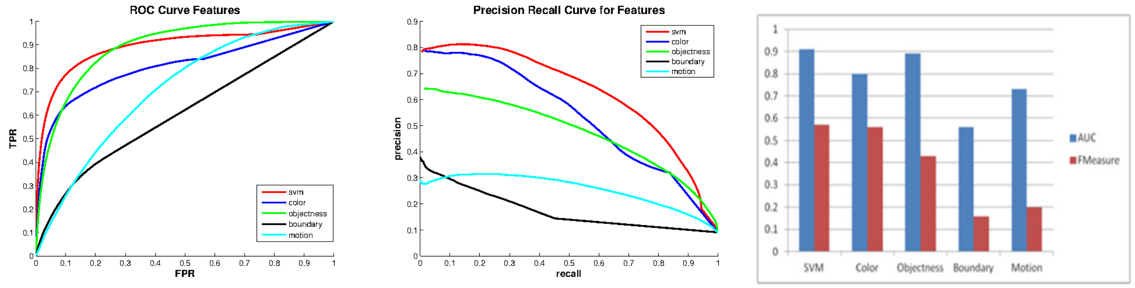

a: ROC curve. b: Precision Recall curve. c: Area under curve (AUC) and F-Measure.

Figure 6: Combination map generated using feature integration (labeled "svm") gives better performance over individual maps.

where w is the weight vector, x_i, l_i are, respectively, the data and label of instance i, C is the penalty parameter, and $\xi(w,b;x_i,l_i)$ is the loss function. These weights give the importance of each feature and they can be viewed as activation functions which enhance certain features and inhibit others. Figure 4 shows the feature integration results.

Learning and updating the weights at each frame using online gradient descent (Karampatziakis and Langford, 2010) is as follows

$$w_{t+1} = w_t - \nabla(w_t x_t l_t) \qquad (9)$$

where w_{t+1} is the weight vector for next frame, w_t is the weight for the current frame and $\nabla(w_t x_t l_t)$ is the loss function. Here the data x_t is the combination map and l_t is the ground truth. Figure 5 shows the process of updating weights.

3.4 Saliency Flow

Video is rich in redundancy in the context of saliency information. Human gaze lasts nearly 5 to 10 frames before shifting in a video (Koffka, 1955). Inter-frame saliency dependence is strong so that a salient superpixel in a current frame is most likely to be salient in the previous frame. This gives us a chain like structure between superpixels ("old superpixels") that exists in a previous frame. An old superpixel may change its size due to perspective change but its boundary remains the same. If a superpixel pops up in the current frame it is called a "new superpixel."

There are many centers of activation in an image which can influence saliency. We extend it to video by finding the center of activation in T previous frames; in our work, we set $T = 5$ corresponding to the lower end of the human gaze duration. For an old superpixel, the activation center is found by finding the most salient superpixel in T previous frames. For a new superpixel we find the closest nearest neighbor which can influence its saliency. A superpixel feature is given by the feature vector $\langle \bar{x}, \bar{y}, \bar{L}, \bar{a}, \bar{b}, tex\rangle$ consisting of the average location, CIE $L{*}a{*}b{*}$ color channel values, and texture information. This feature vector is used for a nearest neighbor search. Figure 7b shows a pictorial reference to this search process. Temporal superpixels give the temporal linkage from which we find the center of activation from a set of previous frames that has the maximum influence on the current superpixel r:

$$mv_r = \begin{cases} \max\limits_{k=1,\cdots,T} S_{r,t-k} & r \in OldSP \\ \max\limits_{k=1,\cdots,T} \hat{S}_{r,t-k} & r \in NewSP \end{cases} \qquad (10)$$

where $S_{r,\tau}$ is the saliency from Equation 7 for the same superpixel in frame τ, $\underset{t\in T}{\hat{S}_{r,\tau}}$ is the value from Equation 7 for the closest superpixel in frame τ, $\tau = t{-}1,\ldots, t{-}T$. The current frame's saliency for superpixl r is updated from the previous frames by

$$SalFlow_r = (S_r + mv_r)/2 \qquad (11)$$

where mv_r is activation center's saliency value found for superpixel r and S_r is the saliency value for the current superpixel r.

4 EXPERIMENTS

Algorithm 1 shows the steps for computing saliency map. Training was done using 10-fold cross validation which resulted in an accuracy of 92.7%. The importance of features found using SVM weight vector is in the following order: objectness, color dissimilarity, boundary score, and motion difference. We test our algorithm on the Segtrack and Fukuchi data sets. Segtrack (Tsai *et al.*, 2012) is widely used

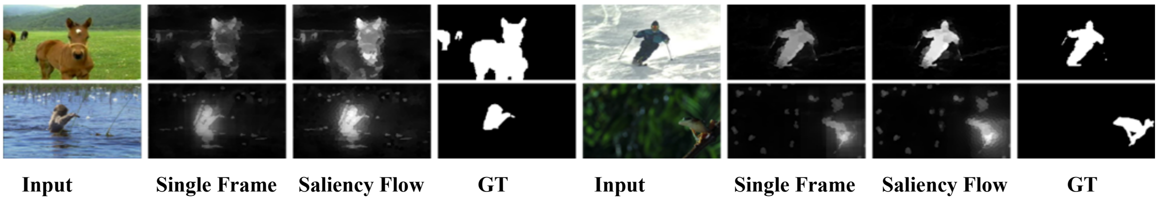

Figure 7a: Saliency Flow improves results over individual frames. "GT" refers to ground truth.

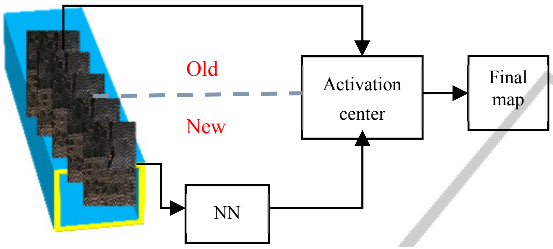

Figure 7b: Search for activation center (Saliency Flow).

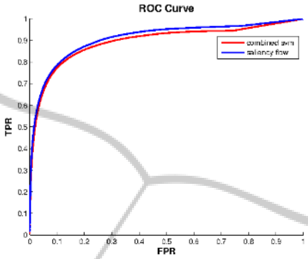

Figure 7c: ROC curve

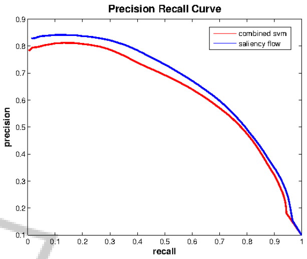

Figure 7d: Precision Recall Curve.

```
Algorithm 1: Video Saliency Detection
1.  Compute temporal superpixels for each frame
    a.  for each superpixel do
        1)  Compute color dissimilarity Eq. 2;
        2)  Compute motion difference Eq. 4;
        3)  Compute objectness Eq. 5;
        4)  Compute boundary score Eq. 6;
2.  Learn weights using linear SVM
        a.  update weights using online gradient decent
        b.  Generate combination map using learned
            weights Eq. 7;
3.  Compute saliency flow to account for temporal
    consistency Eq. 10 ;
4.  Generate final map.
```

for figure-ground segmentation and tracking. It has 16 videos with a total of 976 frames with one or more objects along with such characteristics as motion blur, appearance change, complex deformation, occlusion, slow motion and interacting objects. The Fukuchi *et al.* (2009) dataset has 10 natural scenes videos consisting of 936 frames with one object.

We perform quantitative evaluations to show (i) that feature combination maps out performs individual features, (ii) that saliency flow generates a better saliency map than single frame maps, and (iii) that our method outperforms other state-of-the-art methods.

Evaluation metrics are consistent for all three sets of experiment. We use the benchmark code by Borji *et al.* (2012) to ensure standard evaluations results. We compute the area under the ROC curve. This area shows how well the saliency algorithm predicts against the ground truth. Precision is defined as the ratio of salient object to ground truth, so that the higher the precision the more the saliency map overlaps with the ground truth. The recall measure quantifies the amount of ground truth detected. The weighted harmonic mean measure or F-Measure (Cheng *et al.*, 2011) of precision and recall is given as

$$F = \frac{(1+\beta^2)\cdot precision \cdot recall}{\beta^2 \cdot (precision + recall)} \qquad (12)$$

where β^2 is set at 0.3. The data set used for evaluation is a combination of the Segtrack and Fukuchi data sets. We also perform qualitatively evaluation using example images.

Feature Combination Evaluation: We compute four feature maps and the final integrated map learnt using SVM weights. Figure 6a shows the average ROC curve; Figure 6b shows precision-recall curve; Figure 6c shows the area under curve and the F-Measure. From these plots, we can see that the integrated map out-performs all other feature maps.

Saliency Flow Evaluation: The ROC curve in Figure 7c and the precision-recall curve in Figure 7d as well as the visual comparison in Figure 7a show that saliency flow improves saliency detection.

Comparison to State-of-the-art Methods: In order to compare our work we use ROC curve (Figure 8a), precision-recall curve (Figure 8b) and visual comparison (Figure 9) with other saliency detection methods (Table 1).

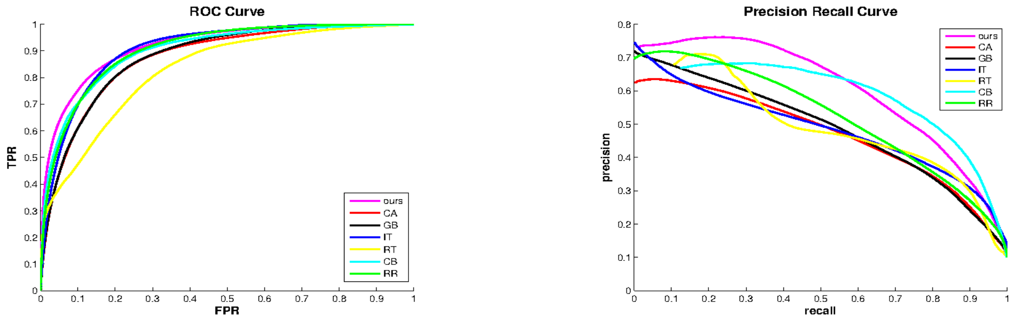

a: ROC curve.

b: Precision Recall curve.

Figure 8: Comparisons of our method ("ours") with other state of art methods (see Table 1) using the ROC and the Precision Recall curves.

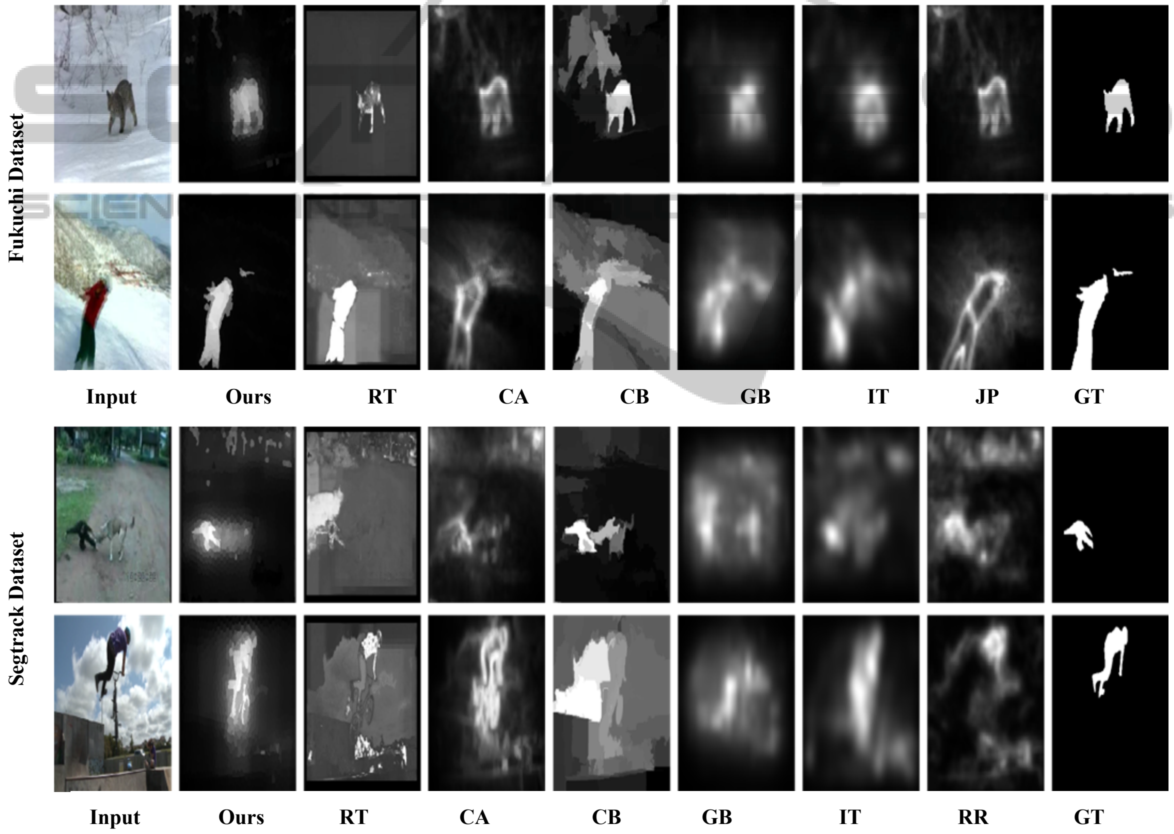

Figure 9: Visual comparisons of our results ("ours") with other state-of-the-art methods. See Table 1 for method references.

Table 1: Saliency detection methods for comparison.

Method	Reference
IT	(Itti and Baldi, 2005)
RR	(Mancas et al., 2011)
JP	(Fukuchi et al., 2009)
RT	(Rahtu et al., 2010)
CA	(Goferman et al., 2010)
CB	(Jiang et al., 2011)
GB	(Harel et al., 2007)

Methods IT, RR, JP and RT are video saliency algorithms while CA, CB are among the best methods that find salient objects (Borji *et al.*, 2012); GB has the best performance among eye-tracking methods. We use the authors' implementations to generate video saliency map for the Fukuchi and Segtrack data sets. From the comparison result we can quantitatively establish that our methods outperform other methods.

5 CONCLUSIONS

We proposed a video saliency detection method based on using SVM to learn weights for combining features represented by superpixel clusters. The process of combining features in the new algorithm performs better than any individual feature. The saliency flow from a video sequence generates a better saliency map than single frame maps. We compared our new method to other state-of-the-art methods using publically available data sets and showed that the new method has better performance. The reported result is the first known application of temporal superpixels for video saliency detection. Our ongoing work is in visual tracking, in which we find the most salient object along with temporal linkage. The saliency map with salient objects can also be used to guide video segmentation.

ACKNOWLEDGMENTS

The authors thank the reviewers whose suggestions improved the manuscript. This work was supported in part by the Louisiana Board of Regents through grant no. LEQSF (2011-14)-RD-A-28.

REFERENCES

Alexe, B., Deselaers, T., and Ferrari, V., 2012. Measuring the objectness of image windows. *IEEE Transactions on PAMI*, vol. 34, no. 11, pp. 2189-2202.

Borji, A., Sihite, D.N., and Itti, L., 2012. Salient object detection: A benchmark. In *ECCV,* pp. 414-429.

Chang, J., Wei, D., and Fisher, J.W., 2013. A video representation using temporal superpixels. In *IEEE CVPR*, pp. 2051-2058.

Chang Y., and Lin, C.-J., 2008. Feature ranking using linear SVM. *JMLR Workshop and Conference Proceedings,* vol. 3, pp. 53-64.

Cheng, M.-M., Zhang, G.-X., Mitra, N.J., Huang, X., and Hu, S.-M., 2011. Global contrast based salient region detection. In *IEEE CVPR*, pp.409-416.

Fukuchi, K., Miyazato, K., Kimura, A., Takagi S., and Yamato, J., 2009. Saliency-based video segmentation with graph cuts and sequentially updated priors. In *ICME*, pp.638-641.

Goferman, S., Zelnik-Manor, L., and Tal, A., 2010. Context-aware saliency detection. In *IEEE CVPR,* pp. 2376-2383.

Grundmann, M., Kwatra, V., Han, M. and Essa, I., 2010. Efficient hierarchical graph-based video segmentation. In *IEEE CVPR*, pp. 2141-2148.

Harel, J., Koch, C., and Perona, P., 2007. Graph-Based Visual Saliency. In *NIPS,* pp. 545-552.

Itti L., and Baldi, P. 2005. A principled approach to detecting surprising events in video. In *IEEE CVPR*, pp. 631-637.

Jiang, H., Wang, J., Yuan, Z., Liu, T., Zheng, N., and Li. S., 2011. Automatic salient object segmentation based on context and shape prior. In *BMVC*, pp 7

Karampatziakis, N., and Langford, J. 2010. Online importance weight aware updates. In *UAI,* pp 392-399.

Koffka, K., 1955. *Principles of Gestalt Psychology*. Routledge & Kegan Paul.

Mahadevan, V., and Vasconcelos, N., 2010. Spatio-temporal saliency in dynamic scenes. *IEEE Transactions on PAMI*, vol. 32, no. 1, pp. 171-177.

Mancas, M., Riche, N., Leroy, J., and Gosselin, B., 2011. Abnormal motion selection in crowds using bottom-up saliency. In *IEEE ICIP*, pp. 229-232.

Mital, P.K., Smith, T.J., Hill, R.L., and Henderson, J.M., 2011. Clustering of gaze during dynamic scene viewing is predicted by motion. *Cognitive Computation*, vol. 3, no. 1, pp. 5-24.

Paris S., and Durand, F., 2007. A topological approach to hierarchical segmentation using mean shift. In *IEEE CVPR*, pp. 1-8.

Rahtu, E,. Kannala, J., Salo, M., and Heikkilä, J., 2010. Segmenting salient objects from images and videos. In *ECCV,* pp. 366-379.

Ren, X., and Bo, L., 2012. Discriminatively trained sparse code gradients for contour detection. In *NIPS*, pp. 584-592.

Ren, X., and Malik, J., 2003. Learning a classification model for segmentation. In *IEEE ICCV*, pp. 10-17.

Reso, M., Jachalsky, J., Rosenhahn, B., and Ostermann, J., 2013. Temporally consistent superpixels. In *IEEE ICCV*, pp. 385-392.

Rudoy, D., Goldman, D.B., Shechtman, E., and Zelnik-Manor, L., 2013. Learning video saliency from human gaze using candidate selection. In *IEEE CVPR*, pp. 1147-1154.

Sharon, E., Galun, M., Sharon, D., Basri, R., and Brandt, A., 2006. Hierarchy and adaptivity in segmenting visual scenes. *Nature*, vol. 442, no. 7104, pp.719-846.

Singh, A., Chu, C.H., Pratt, M.A., 2014. Multiresolution superpixels for visual saliency detection. In *IEEE Symposium on Computational Intelligence for Multimedia, Signal, and Vision Processing.*

Sun, J., and Ling, H., 2013. Scale and object aware image thumbnailing. *International Journal of Computer Vision*, vol. 104, no. 2, pp. 135-153.

Sun, D., Roth, S., and Black, M.J., 2010. Secrets of optical flow estimation and their principles. In *IEEE CVPR*, pp. 2432-2439.

Treisman, A.M., and Gelade. G., 1980. A feature-integration theory of attention. *Cognitive Psychology,* vol 12, no. 1, pp 97-136.

Tsai, D., Flagg, M., Nakazawa, A., and Rehg, J.M., 2012. Motion coherent tracking using multi-label MRF optimization. *International Journal of Computer Vision* vol. 100, no.2, pp. 190-202.

Van den Bergh, M., Roig, G., Boix, X., Manen, S., and Van Gool, L., 2013. Online video seeds for temporal window objectness. In *IEEE ICCV*, pp. 377-384.

Veksler, O., Boykov, Y., and Mehrani, P., 2010. Superpixels and supervoxels In an energy optimization framework. In *ECCV*, pp. 211-224.

Xu, C., and Corso, J.J., 2012. Evaluation of super-voxel methods for early video processing. In *IEEE CVPR*, pp. 1202-1209.